

Application of stoichiometric CT number calibration method for dose calculation of tissue heterogeneous volumes in boron neutron capture therapy

Naonori Hu^{1,2} | Minoru Nakao^{3,4} | Shuichi Ozawa^{3,4} | Takushi Takata¹ | Hiroki Tanaka¹ | Keiji Nihei^{2,5} | Koji Ono² | Minoru Suzuki¹

¹Institute for Integrated Radiation and Nuclear Science, Kyoto University, Sennangun, Osaka, Japan

²Kansai BNCT Medical Center, Osaka Medical and Pharmaceutical University, Takatsuki, Osaka, Japan

³Hiroshima High-Precision Radiotherapy Cancer Center, Hiroshima, Japan

⁴Department of Radiation Oncology, Hiroshima University, Hiroshima, Japan

⁵Department of Radiation Oncology, Osaka Medical and Pharmaceutical University Hospital, Takatsuki, Osaka, Japan

Correspondence

Naonori Hu, Kansai BNCT Medical Center, Osaka Medical and Pharmaceutical University, Takatsuki, Osaka, Japan.
Email: naonori.ko@ompu.ac.jp

Funding information

Japan Society for the Promotion of Science, Grant/Award Number: 23K14869

Abstract

Background: Monte Carlo simulation code is commonly used for the dose calculation of boron neutron capture therapy. In the past, dose calculation was performed assuming a homogeneous mass density and elemental composition inside the tissue, regardless of the patient's age or sex. Studies have shown that the mass density varies with patient to patient, particularly for those that have undergone surgery or radiotherapy. A method to convert computed tomography numbers into mass density and elemental weights of tissues has been developed and applied in the dose calculation process using Monte Carlo codes. A recent study has shown the variation in the computed tomography number between different scanners for low- and high-density materials.

Purpose: The aim of this study is to investigate the effect of the elemental composition inside each calculation voxel on the dose calculation and the application of the stoichiometric CT number calibration method for boron neutron capture therapy planning.

Methods: Monte Carlo simulation package Particle and Heavy Ion Transport code System was used for the dose calculation. Firstly, a homogeneous cubic phantom with the material set to ICRU soft tissue (four component), muscle, fat, and brain was modelled and the NeuCure BNCT system accelerator-based neutron source was used. The central axis depth dose distribution was simulated and compared between the four materials. Secondly, a treatment plan of the brain and the head and neck region was simulated using a dummy patient dataset. Three models were generated; (1) a model where only the fundamental materials were considered (simple model), a model where each voxel was assigned a mass density and elemental weight using (2) the Nakao20 model, and (3) the Schneider00 model. The irradiation conditions were kept the same between the different models (irradiation time and irradiation field size) and the near maximum ($D_{1\%}$) and mean dose to the organs at risk were calculated and compared.

Results: A maximum percentage difference of approximately 5% was observed between the different materials for the homogeneous phantom. With the dummy patient plan, a large dose difference in the bone (greater than 12%) and region near the low-density material (mucosal membrane, 7%–11%) was found between the different models.

This is an open access article under the terms of the [Creative Commons Attribution](https://creativecommons.org/licenses/by/4.0/) License, which permits use, distribution and reproduction in any medium, provided the original work is properly cited.

© 2024 The Authors. *Medical Physics* published by Wiley Periodicals LLC on behalf of American Association of Physicists in Medicine.

Conclusions: A stoichiometric CT number calibration method using the newly developed Nakao20 model was applied to BNCT dose calculation. The results indicate the importance of calibrating the CT number to elemental composition for each individual CT scanner for the purpose of BNCT dose calculation along with the consideration of heterogeneity of the material composition inside the defined region of interest.

KEYWORDS

BNCT, Monte Carlo Simulation, Stoichiometric CT number calibration

1 | INTRODUCTION

Boron neutron capture therapy (BNCT) is a type of particle therapy which utilizes a neutron beam with ^{10}B containing drug to treat patients with cancer. The principal of BNCT is the local energy deposition by the alpha particles and ^7Li ions produced from the thermal neutron capture reaction, $^{10}\text{B}(n,\alpha)^7\text{Li}$.¹ In addition, protons are generated from the thermal neutron capture reaction of nitrogen atoms $^{14}\text{N}(n,p)^{14}\text{C}$ and fast neutrons causing recoil protons from hydrogen in tissue. Furthermore, gamma rays are produced from the thermal neutron capture reaction of hydrogen atoms $^1\text{H}(n,\gamma)^2\text{H}$ and from the primary beam itself. To accurately determine the dose delivered the contribution of each of the above components should be considered. In addition, the mass, dimension, and elemental composition of the organs and tissues are required^{2,3} along with the neutron energy spectrum and fluence at each location. Given the complexity of the dose calculation, Monte Carlo simulation programs are utilized to estimate the dose deposited in each organ and tissue. The conventional method has been to simplify a few region model (soft tissue, bone, air) or use a spatially homogenized model to generate the patient geometry.^{4–6} Moran et al., investigated the geometric heterogeneity effects in radiation dose distribution for BNCT of canine brain tumours.⁷ This study showed there was a difference of 10%–20% in the neutron and photon flux magnitude in the regions of the brain near the sinus cavities. This was due to the spatial shift of the thermal neutron flux peak because the heterogeneous model accurately represents the sinus void region, which can be therapeutically significant and a need for proper validation of simplified treatment planning models is required. To obtain the composition data for modelling, Moran et al. performed actual dissections of the canine head and chemical analyses were performed on all tissue samples to determine the elemental composition, as a comprehensive canine tissue composition information was not available. Data on reference human tissues are available but International Commission on Radiological Protection (ICRP) report 89 states that for some parameters there are large differences in the values between certain populations and the indicated refer-

ence values. For instance, the mass of fat in an adult male from China has a difference of around 50% of the reference value stated in the report.³ A need to determine the elemental composition and weight of each tissue for each individual patient is ideal for accurate dose calculation. One of the methods to achieve this is to perform a computed tomography (CT) scan of a patient and convert the CT number to mass density and elemental weights of standard tissues using stoichiometric CT number calibration method.^{8,9} This method generates a relationship between CT number and mass density/elemental weights using a multiparameter fit and the theoretical CT numbers for standard tissues are calculated from the obtained fitting parameters. The work by Wilfried Schneider et al., serves as a reference database for determination of tissue mass density and elemental weights from CT numbers.⁹ Several studies have compared stoichiometric CT number calibration with a tissue substitute CT number calibration for photon and proton radiotherapy treatment planning.^{10–13} The current BNCT treatment planning process utilises a “simple method”, where the mass density and elemental composition of the defined regions (region of interest: ROI) are set and assumed to be a homogeneous material composition.^{14,15} Some studies have applied voxel-by-voxel dose calculation method where the CT images are converted into a voxel phantom and each individual voxel is assigned an elemental composition, but have either directly used the Schneider database,¹⁶ or have used their own CT number to material conversion process without information on the fine details on the process and how the CT numbers were calibrated.^{17–19} In a recent study by Teng et al., they have developed a CT number based material conversion to perform accurate BNCT dose calculation.²⁰ They also mention the importance of defining the voxel material in the region of interest (inter-region of interest) but have performed the CT number to tissue density and material composition calibration using the Schneider database.

Nakao et al., developed a new stoichiometric CT number calibration model (Nakao20 model) which utilizes a three parameter fit model to generate a unique tissue mass density and elemental weight table based on the CT images acquired at the hospital/institute to

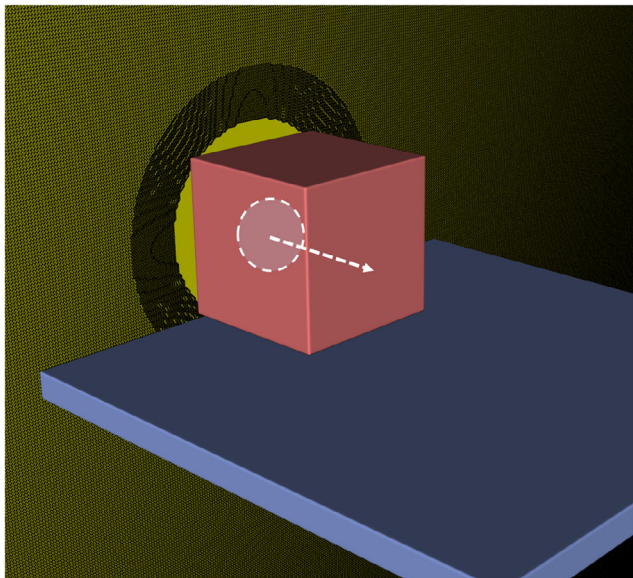


FIGURE 1 Geometry of the cubic phantom modelled using PHITS. The material was set to soft tissue, muscle, adipose, and brain. PHITS, Particle and Heavy Ion Transport code System

account for the difference in the x-ray tube voltage. This method has been applied to high energy photon and proton therapy, but not for BNCT planning. Recently, it has been reported that this methodology has shown to improve the CT number calibration for low density tissues.²¹

This study aims to investigate the elemental composition effect on the dose distribution in BNCT and introduce a simple method for calibrating and converting the CT number into elemental composition and weight using the Nakao20 model for the purpose of BNCT dose calculation.

2 | METHODS

2.1 | Homogeneous phantom simulation

The central axis thermal neutron and absorbed dose distribution inside a homogeneous cubic phantom (20 cm × 20 cm × 20 cm, Figure 1) was simulated using the Particle and Heavy Ion Transport code System (PHITS version 3.26) Monte Carlo simulation package.²² The material composition inside the cubic phantom was set to ICRU four component soft tissue, adipose, muscle, and brain. The elemental composition and density of each material are summarized in Table 1 and were adopted from ICRP publication 110.²³ Individual simulation was performed for each material. The neutron and photon source of the NeuCure BNCT System, which has been previously evaluated,¹⁵ was used and the absorbed dose was calculated by multiplying the simulated neutron and photon energy spectrum with the

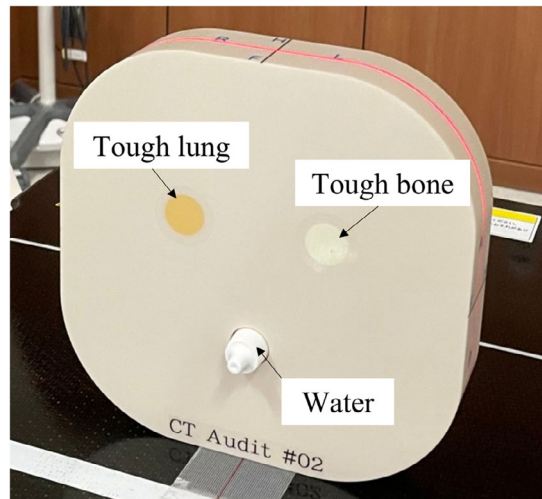


FIGURE 2 CT number calibration audit phantom designed by Hiroshima High Precision Radiotherapy Cancer Center manufactured by Taisei Medical Co., Ltd.

kinetic energy released in matter (KERMA) coefficient (see appendix).

2.2 | Stoichiometric CT number calibration

A CT scan of the CT number calibration audit phantom (designed by the researchers at Hiroshima High-Precision Radiotherapy Cancer Center and manufactured by Taisei Medical Co., Ltd, Osaka, Japan (Figure 2) was performed using the parameters summarized in Table 2. The phantom consisted of three plugs, tough lung, tough bone, and water and the surrounding material consisted of a water-equivalent material. The measured CT number, along with the known mass density and elemental composition of each plug, was used to determine the fitting parameters. Detail of the CT number calibration using the fitting parameters can be found in the appendix.

The CT number to mass density calibration tables were created using a combination of the 11 representative tissues (summarized in Table A1), defined by Kanematsu et al.,²⁴ (which were derived from the adult reference computational phantom data ICRP 110²³) and the ICRU 46 lung material. Miscellaneous is defined as the volume-weighted mean of epithelium, connective, and spongy-bone tissue. The theoretical CT numbers for the 12 representative tissues were calculated using the three parameters, α , k_1 , and k_2 , 1.24×10^{-3} , 3.06×10^{-5} , and 1.0, respectively. To determine the tissue parameters (mass density, ρ , and elemental weight, w_j) for CT numbers between heavy spongiosa and mineral bone, an interpolation method defined by Schneider et al.,⁹ was used. The tissue parameters defined by

TABLE 1 Density and elemental composition from ICRP 110.²³

Material	Density (g/cm ³)	H	C	N	O	Res
Tissue soft	1.00	0.102	0.456	0.035	0.407	—
Adipose	0.95	0.114	0.598	0.007	0.278	0.003 ^a
Muscle	1.05	0.102	0.143	0.034	0.710	0.011 ^b
Brain	1.04	0.107	0.145	0.022	0.712	0.014 ^c

Abbreviation: ICRP, International Commission on Radiological Protection.

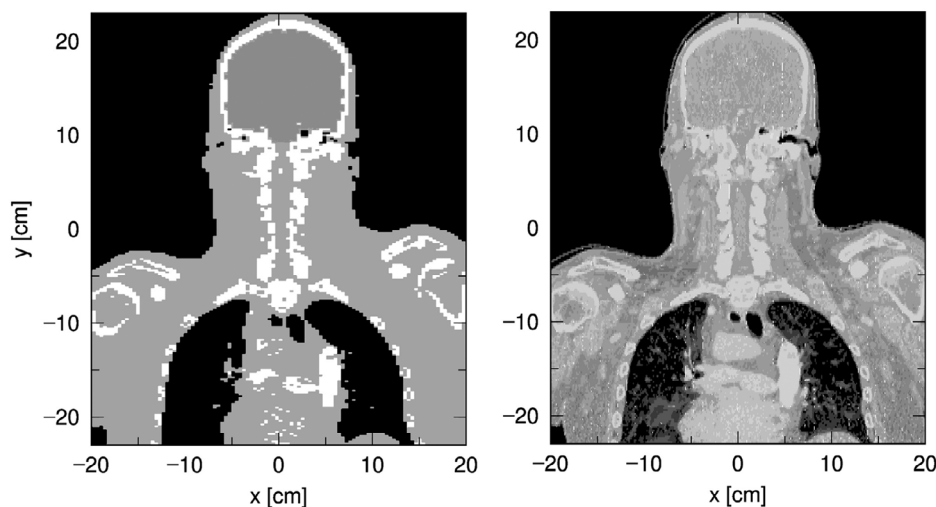
^a0.001 Na, 0.001 S, 0.001 Cl.

^b0.001 Na, 0.002 P, 0.003 S, 0.001 Cl, 0.004 K.

^c0.002 Na, 0.004 P, 0.002 S, 0.003 Cl, 0.003 K.

TABLE 2 CT scanner parameter used to scan the CT number calibration audit phantom.

CT scanner	Scan protocol	Tube voltage (kVp)	Slice thickness (mm)	Scan field of view (mm)	Display field of view (mm)	Scan method
Canon AquilionLB	Head and neck	120	2	400	400	Helical

**FIGURE 3** Coronal view of the voxel model generated using RTphits module for the simple model (left) and the voxel-by-voxel model using Nakao20 method (right).

Schneider et al.,⁹ (here named Schneider00) was also used for comparison.

2.3 | 3D dose distribution using a dummy patient dataset

A CT dataset of a dummy patient used for training and education purposes for the head and neck region (provided by RaySearch Laboratories, CT scanner information was not provided) was used. The CT images were converted into a voxel phantom using RTphits module of PHITS (Figure 3). The DICOM (Digital Imaging and Communications in Medicine) header information (pixel size, slice thickness, number of slices, etc.) of the CT images were extracted and the 3D voxel data was generated into a PHITS-input file (lattice) format. To reduce the processing time, the lattice file was

converted into a binary file format. The CT number to mass density calibration table (see previous section) was used to assign the mass density and elemental composition of each voxel.

Three different models were prepared; (1) a simple model where only the air, soft tissue, brain, and bone (based on the ICRP 110) were considered, (2) a voxel-by-voxel model using the Schneider00 database (originally calibrated using the Siemens Somatom Plus 4 CT scanner), and (3) a voxel-by-voxel model using the Nakao20 method (calibrated using the Canon AquilionLB CT scanner at the Kansai BNCT Medical Center). The ¹⁰B concentration inside each voxel was assumed to be 25 ppm, except for voxels with a CT number less than -984 HU (i.e., air) where a value of 0 ppm was set. Three different cases were considered, BNCT of the brain, BNCT of the nasopharynx, and BNCT of the hypopharynx region (Figure 4). The organs at

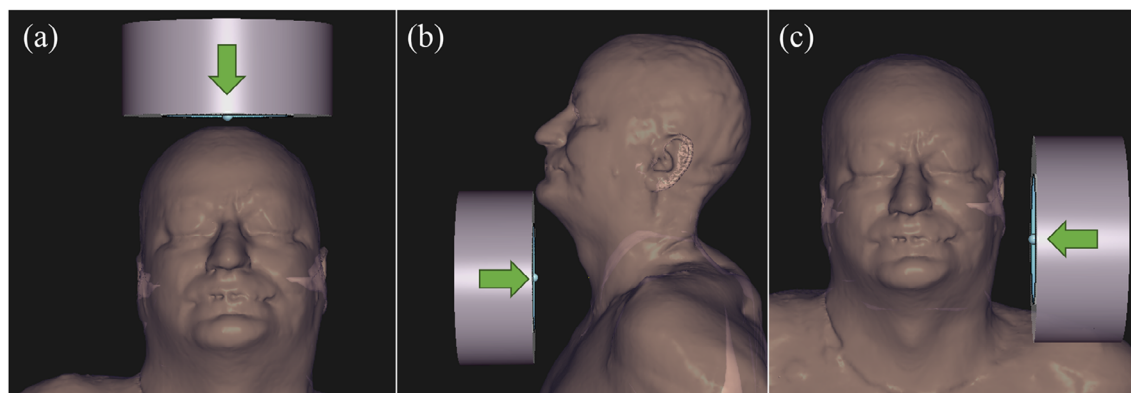


FIGURE 4 Three BNCT irradiations were considered in this study. (a) BNCT of the brain with the neutron beam entering from the vertex of the patient, (b) BNCT of the larynx with the neutron beam entering from the front of the patient, and (c) BNCT of the left parotid with the neutron beam entering from the left side of the patient. All simulations were performed with the standard 12 cm circular diameter collimator with an irradiation time of 1 h.

risk (OAR) were defined using RayStation version 9A. The OARs defined for the brain treatment were the brain, brainstem, spinal cord, eyes, mandible, and skin. The cranial bone is not considered as an OAR but the dose delivered to this region was also calculated. For the nasopharynx and hypopharynx treatment, the OARs were the same as above, with the addition of the esophagus, mucosa, lungs, parotid glands, and thyroid. Most of the OARs (brain, brainstem, spinal cord, eyes, mandible, parotid glands, thyroid, lungs) were defined using the model based segmentation function of RayStation. The bone and air regions were generated using gray level threshold settings (bone ≥ 150 HU, air ≤ -250 HU). The generated structure set was used for the evaluation of all three models. The neutron source of the NeuCure BNCT system was used with a 12 cm diameter circular field size. The calculation mesh size was set to 2 mm^3 and the total number of particles were kept the same for all simulations (1×10^{10}). A mesh size of 2 mm^3 was assigned in alignment with the current clinical recommendation²⁵ and the total number of particles were assigned to be the same as a previous study, where the relative uncertainty in the thermal neutron and gamma ray flux was below 0.5% and 1%, respectively.¹⁵ Simulations were performed using PHITS and a comparison of the absorbed dose was performed using an open-source software, 3D slicer. The irradiation time was assumed to be the same for all cases (1 h). The Japanese Evaluated Nuclear Data Library (JENDL 4.0) developed by Japan Atomic Energy Agency (JAEA) was used.²⁶ Firstly, the dose distribution between the simple model and the voxel-by-voxel models (Nakao20 and Schneider00) were compared to assess the impact of the difference in the dose distribution when inter-ROI material composition heterogeneity was considered. Secondly, the comparison between Nakao20 model and Schneider00 database was performed to assess the difference in the dose calculation

between a generic CT-material composition table (Schneider00 database) and a unique scanner-specific CT-material composition table (Nakao20 model) and whether if there is a need for generating individual CT number to material composition table for BNCT dose planning.

3 | RESULT

3.1 | Uniform phantom simulation

The central axis depth distribution of the total dose simulated using PHITS for the different materials is shown in Figure 5. When compared with soft tissue, a maximum absolute difference of 0.53 Gy/h was observed near the surface of the phantom (depth of approximately 1 cm). The central axis dose distribution for each individual dose component is shown in the [appendix](#).

3.2 | Stoichiometric CT number calibration

The mean HU value and the standard deviation for the three plugs was measured to be 1.17 ± 5.27 (water), -641.86 ± 5.98 (tough lung) and 852.44 ± 9.47 (tough bone). The fitting parameters were determined using the equations outlined in the [appendix](#) and the CT number to mass density and elemental composition were determined (Figure A1 and Table A1).

3.3 | 3D dose distribution

The difference in the near maximum dose ($D_{1\%}$) and mean dose (D_{mean}) of the OARs between the

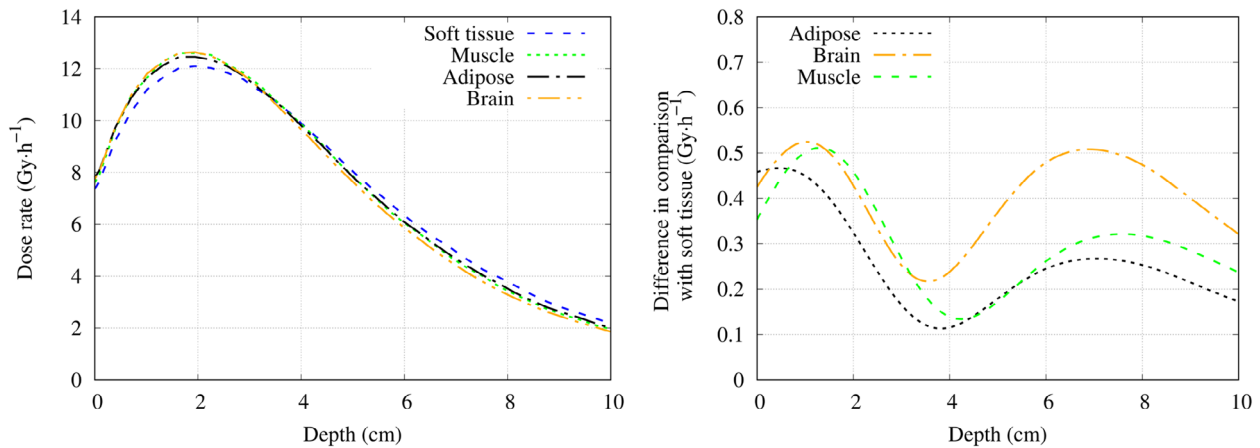


FIGURE 5 (Left) Central axis depth dose rate distribution of the summation of the individual dose component of the different materials. (Right) The dose rate difference compared with soft tissue.

TABLE 3 Dose difference between the simple material model and the voxel-by-voxel model for case 1 (BNCT of the head).

Structure	D _{1%} (Gy)			D _{mean} (Gy)		
	Simple	Voxel-by-voxel (Schneider00)	Voxel-by-voxel (Nakao20)	Simple	Voxel-by-voxel (Schneider00)	Voxel-by-voxel (Nakao20)
Brain	11.0	11.0	11.1	3.3	3.3	3.3
Brainstem	2.1	2.0	2.1	1.2	1.2	1.2
Bone	12.4	9.7	10.0	2.8	2.2	2.2
Eye_L	1.9	1.9	1.9	1.2	1.2	1.2
Eye_R	1.8	1.9	1.9	1.2	1.2	1.2
Mandible	1.3	0.8	0.9	0.7	0.4	0.4
Spinalcord	0.7	0.5	0.5	0.4	0.3	0.4
Skin	10.9	10.4	10.6	2.7	2.6	2.6

Abbreviation: BNCT, boron neutron capture therapy.

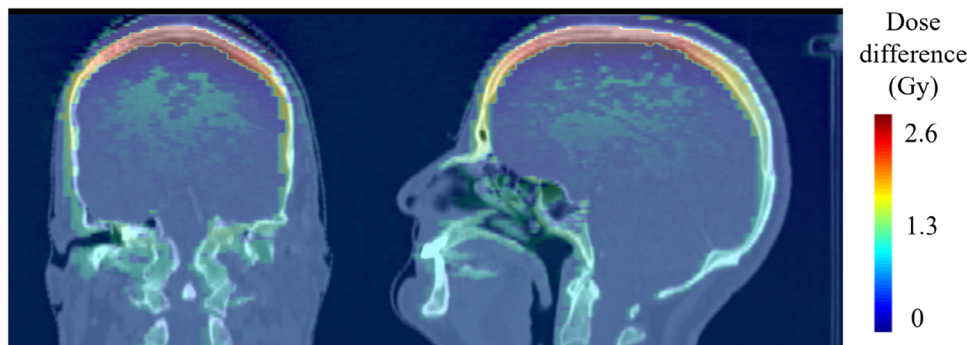


FIGURE 6 2D isodose map showing the dose difference between the simple model and the Nakao20 model for the BNCT of the brain. BNCT, boron neutron capture therapy.

simple model and the voxel-by-voxel model for the head, hypopharynx, and nasopharynx irradiation is shown in Table 3, Table 4, and Table 5, respectively. The total uncertainty in the D_{1%} and D_{mean} was below 0.001 and 0.01 Gy, respectively. The 2D isodose difference map for the BNCT of a brain is shown in Figure 6.

4 | DISCUSSION

Monte Carlo simulations were performed to investigate the impact of various material compositions on the dose distribution for BNCT treatment planning. Firstly, the central axis depth dose distribution inside a homogeneous cubic phantom was simulated. A dose rate difference of

TABLE 4 Dose difference between the simple material model and the voxel-by-voxel model for case 2 (BNCT of the larynx area).

Structure	D _{1%} (Gy)			D _{mean} (Gy)		
	Simple	Voxel-by-voxel (Schneider00)	Voxel-by-voxel (Nakao20)	Simple	Voxel-by-voxel (Schneider00)	Voxel-by-voxel (Nakao20)
Brain	1.2	1.1	1.0	0.4	0.4	0.4
Brainstem	1.4	1.1	1.1	0.8	0.8	0.8
Esophagus	5.0	4.5	4.5	3.2	3.1	3.1
Eye_L	1.3	1.3	1.2	1.0	1.0	1.0
Eye_R	1.5	1.4	1.3	1.0	1.0	1.0
Lung	2.2	1.8	2.3	1.0	0.7	0.9
Parotid_L	2.2	2.3	2.2	1.2	1.3	1.3
Parotid_R	2.6	2.5	2.4	1.5	1.5	1.5
Mandible	5.3	4.4	4.5	3.6	2.8	2.9
Mucosa	7.6	7.3	7.9	3.3	2.6	3.1
Spinalcord	3.6	3.1	3.1	2.1	2.0	1.9
Skin	4.2	4.1	4.2	1.0	0.9	1.0
Thyroid	5.2	5.2	5.3	4.4	4.6	4.7

Abbreviation: BNCT, boron neutron capture therapy.

TABLE 5 Dose difference between the simple material model and the voxel-by-voxel model for case 3 (BNCT of the left parotid area).

Structure	D _{1%} (Gy)			D _{mean} (Gy)		
	Simple	Voxel-by-voxel (Schneider00)	Voxel-by-voxel (Nakao20)	Simple	Voxel-by-voxel (Schneider00)	Voxel-by-voxel (Nakao20)
Brain	6.3	6.3	6.3	1.9	1.9	1.8
Brainstem	4.6	3.7	3.7	2.8	2.6	2.6
Esophagus	1.5	1.5	1.5	0.8	0.8	0.7
Eye_L	1.1	1.1	1.1	0.7	0.7	0.7
Eye_R	2.3	2.4	2.4	1.6	1.7	1.7
Parotid_L	1.1	1.1	1.0	0.6	0.6	0.6
Parotid_R	7.3	7.6	7.4	5.8	6.1	6.0
Mandible	8.4	6.9	7.0	2.6	2.0	2.0
Mucosa	4.6	3.7	4.1	2.1	1.6	1.7
Spinalcord	4.1	3.3	3.3	1.7	1.6	1.5
Skin	5.7	5.7	5.7	1.2	1.2	1.2
Thyroid	2.1	2.1	2.1	1.3	1.3	1.2

Abbreviation: BNCT, boron neutron capture therapy.

approximately 0.5 Gy/h at 1 cm depth and 0.3 Gy/h at a depth of 10 cm was observed between the brain/muscle when compared with ICRU soft tissue. The individual dose components showed the nitrogen dose varied the most between the different tissue types, due to the relatively large differences in the number of nitrogen atoms between each tissue types. Although the boron concentration was kept the same between the different tissues, the boron dose distribution varied slightly. This indicated the neutron distribution inside the phantom was different

for the different tissue types, due to the differing hydrogen atom content and physical density of the material. Therefore, it is important to assign both the physical density and the elemental composition of the material to perform an accurate simulation of the neutron transport. Also, considering the fact BNCT is usually performed in a single fraction, the above stated dose difference would be higher when converted to biologically effective dose (BED), which indicates more of a reason to accurately assign the material composition, particularly if a patient

has received previous external beam radiation therapy and evaluation of the dose to the surrounding OARs becomes critical.

Inside the human body, there are various types of tissues with differing physical densities and elemental compositions. Additionally, these differ from patient to patient, especially those that have undergone surgery, who make up for the majority of patients receiving BNCT.²⁷ Assigning the physical density and the elemental composition for each individual voxel is laborious. Particularly for the bone region where there is a mixture of soft and hard bone, where the simulation results indicated a large difference in dose, up to a percentage difference of 12%. Furthermore, not all tissues are precisely modelled in the treatment planning process. The four primary tissue types (nervous, muscle, epithelial, connective) should be individually assigned for accurate neutron transport simulation.

For the treatment of the brain, the dose is usually prescribed to the scalp or the healthy brain²⁸ and for head and neck the dose is usually prescribed to the mucosal membrane.²⁹ A percentage difference of up to 7% was found between the simple model and the voxel-by-voxel method (Nakao20) for the mucosal membrane. The Nakao20 and Schneider00 calculation results were compared and a noticeable difference at $D_{1\%}$ was found for the bone, lung, and mucosa structures. It has been reported that for high- and low-density tissues, the conventional stoichiometric CT number calibration (Schneider00 method) is not appropriate or errors are introduced from forcing the fitting parameters.³⁰ The CT number to material density curve calculated using the two different methods is shown in the appendix (Figure A1). Few studies have shown the variation in the CT number between different CT scanners and filters used during reconstruction.^{31,32} A study by Cropp et al., showed the CT number of the bone-equivalent plug (ACR phantom) varied between 850–1400 HU, which equated to a physical density of approximately 1.7–2.8 g/cm³.³¹ Coxson investigated the effect of different CT reconstruction algorithms and found a large variation in the CT number in the low-density region.³² A study by Van Dyk et al., showed the variation in the lung density varied with both the age (0.36–0.22 g/cm³) and during inspiration and expiration (0.36–0.20 g/cm³). The impact of the above change in density on the dose distribution is shown in the appendix. Taking both extremities, a maximum dose difference of 6% and 14% was calculated for the lung and bone region, respectively. This shows that for accurate neutron transport and dose calculation of BNCT, calibration of the CT scanner (HU units to physical density) used for acquiring the images for the treatment planning is necessary. It is important to note that, in this study, direct comparison between Nakao20 and Schneider00 calibration method cannot be performed, as mentioned in the introduction, the Nakao20 method was calibrated using the CT scanner

at the Kansai BNCT Medical Center (Canon AquilionLB), whereas the Schneider00 database was originally produced using the Siemens Somatom Plus 4 CT scanner. Therefore, it is difficult to state whether the Nakao00 method is superior to the Schneider method, but the above literature indicates that the CT number should be calibrated at each institute and the direct use of the Schneider database for Monte Carlo dose calculation for BNCT planning should be avoided.

In the future, BNCT may become available for breast and lung cancer, where large areas of low-density regions exist. A planning study performed by Sato et al., showed a difference of up to 20% in the physical density between a healthy lung and a diseased lung (malignant pleural mesothelioma) and the BNCT dose was overestimated if the standard ICRU values were used instead of the true physical density.³³ Furthermore, centers and hospitals offering BNCT is increasing worldwide and a need for a proper protocol to evaluate dose is required for accurate determination of clinical outcome. A universal method for calibration of CT number to mass density and elemental weight may become necessary in the future.

Using the proposed calibration process, the assignment of elemental compositions for each individual voxel can be performed with ease. However, there are some limitations to this study and issues that needs to be considered:

1. The ¹⁰B concentration and distribution inside the body was assumed to be constant and uniformly distributed throughout. There are numerous studies that indicate the boron concentration is non-uniform between tissue types and cancer types.^{34,35} In clinical practice, a common approach to calculate the biologically weighted dose is by using a compound biological effectiveness (CBE) factor, which is the product of the relative biological effectiveness (RBE) and the boron distribution. However, RBE and CBE concepts are only applicable under clearly specified conditions.³⁶ For accurate dose calculation, a method to determine the ¹⁰B concentration inside each calculation voxel is required, such as using FBPA-PET (¹⁸F fluoro-phenylalanine) images.
2. Low energy neutron scattering is sensitive to the atomic structure of a material. To accurately simulate the thermal neutron distribution, the thermal neutron scattering law data, $S(\alpha,\beta)$, for water at room temperature was used for all tissues. Currently, there is no data available for human tissues.
3. As the elemental composition and physical density is based on the CT number, the image quality is crucial for accurate dose calculation. The elemental composition assignment for artificial materials (such as dental implants, surgical clips, and pacemakers) cannot be performed with the proposed method. The elemental composition and physical density will need

to be set manually for these materials. Furthermore, CT artifacts (e.g., streak artifacts) will need to be corrected before applying the stoichiometric CT number calibration.

4. Materials with similar CT numbers, such as calcified plaques and iodine-containing blood, differ considerably in atomic number but may appear identical on a CT scan, resulting in the same mass density and elemental composition. A potential method to overcome this issue is by using a multi-energy CT to differentiate between the two materials.
5. Since this is purely a simulation study, an experimental study is necessary to validate the work presented here. The future work will include preparing a heterogeneous phantom and performing experimental measurements under different conditions and comparing it with the Nakao20 model.

5 | CONCLUSION

A stoichiometric CT number calibration method was applied for the BNCT dose calculation. A large deviation (greater than 12% at $D_{1\%}$) between the simple model and the voxel-by-voxel calibration method (Nakao20) was observed for the bone structure. A percentage difference of 2.8% and 11.5% was observed between the two models for the skin and the mucosal membrane of the brain and left parotid BNCT irradiation, respectively. This study showed the heterogeneous elemental composition inside the human body, particularly regions where the change is dramatic (air-tissue, air-bone), should be carefully defined and the calibration of CT number to mass density/elemental composition should be performed for each individual CT scanner for accurate BNCT dose calculation.

ACKNOWLEDGMENTS

This research was partly supported by JSPS KAKENHI (Japan Society for the Promotion of Science Grants-in-Aid for Scientific research) Grant Number 23K14869.

CONFLICT OF INTEREST STATEMENT

The authors have no relevant conflicts of interest to disclose.

REFERENCES

1. Locher GL. Biological effects and therapeutic possibilities of neutrons. *Am J Roentgenol Radium Ther.* 1936;36:1-13.
2. ICRP. *Report on the Task Group on Reference Man.* ICRP Publication 23. Pergamon Press; 1975.
3. Ann ICRP. Basic anatomical and physiological data for use in radiological protection: reference values. ICRP Publication 89. *Ann ICRP.* 2002;32(3-4):5-265. <http://www.ncbi.nlm.nih.gov/pubmed/14506981>
4. Nigg DW. Computational dosimetry and treatment planning considerations for neutron capture therapy. *J Neurooncol.* 2023;62(1-2):75-86.
5. Kumada H, Takada K, Aihara T, Matsumura A, Sakurai H, Sakae T. Verification for dose estimation performance of a Monte-Carlo based treatment planning system in University of Tsukuba. *Appl Radiat Isot.* 2020;166:109222. doi:10.1016/j.apradiso.2020.109222
6. Kumada H, Nakamura T, Komeda M, Matsumura A. Development of a new multi-modal Monte-Carlo radiotherapy planning system. *Appl Radiat Isot.* 2009;67(7-8):118-121. doi:10.1016/j.apradiso.2009.03.028
7. Moran JM, Nigg DW, Wheeler FJ, Bauer WF. Macroscopic geometric heterogeneity effects in radiation dose distribution analysis for boron neutron capture therapy. *Med Phys.* 1992;19(3):723-732. doi:10.1118/1.596816
8. Schneider U, Pedroni E, Lomax A. The calibration of CT Hounsfield units for radiotherapy treatment planning. *Phys Med Biol.* 1996;41(1):111-124. doi:10.1088/0031-9155/41/1/009
9. Schneider W, Bortfeld T, Schlegel W. Correlation between CT numbers and tissue parameters needed for Monte Carlo simulations of clinical dose distributions. *Phys Med Biol.* 2000;45(2):459-478. doi:10.1088/0031-9155/45/2/314
10. Johannes I, Kolditz D, Langner O, Kalender WA. A formulation of tissue- and water-equivalent materials using the stoichiometric analysis method for CT-number calibration in radiotherapy treatment planning. *Phys Med Biol.* 2012;57(5):1173-1190. doi:10.1088/0031-9155/57/5/1173
11. Vanderstraeten B, Chin PW, Fix M, et al. Conversion of CT numbers into tissue parameters for Monte Carlo dose calculations: a multi-centre study. *Phys Med Biol.* 2007;52(3):539-562. doi:10.1088/0031-9155/52/3/001
12. Martinez LC, Calzado A, Rodriguez C, Gilarranz R, Manzananas MJ. A parametrization of the CT number of a substance and its use for stoichiometric calibration. *Phys Medica.* 2012;28(1):33-42. doi:10.1016/j.ejmp.2011.02.001
13. Ödén J, Zimmerman J, Poludniowski G. Comparison of CT-number parameterization models for stoichiometric CT calibration in proton therapy. *Phys Medica.* 2018;47:42-49. doi:10.1016/j.ejmp.2018.02.016
14. Kato R, Hirose K, Kato T, et al. Dosimetric effects of the ipsilateral shoulder position variations in the sitting-positioned boron neutron capture therapy for lower neck tumor. *Appl Radiat Isot.* 2022;188:110397. doi:10.1016/j.apradiso.2022.110397
15. Hu N, Tanaka H, Kakino R, et al. Evaluation of a treatment planning system developed for clinical boron neutron capture therapy and validation against an independent Monte Carlo dose calculation system. *Radiat Oncol.* 2021;16(1):1-13. doi:10.1186/s13014-021-01968-2
16. Lee CM, Lee HS. Development of a dose estimation code for BNCT with GPU accelerated Monte Carlo and collapsed cone Convolution method. *Nucl Eng Technol.* 2022;54(5):1769-1780. doi:10.1016/j.net.2021.11.010
17. González SJ, Carando DG, Santa Cruz GA, Zamenhof RG. Voxel model in BNCT treatment planning: performance analysis and improvements. *Phys Med Biol.* 2005;50(3):441-458. doi:10.1088/0031-9155/50/3/004
18. Kumada H, Yamamoto K, Hong LP, Matsumura A, Nakagawa Y. Improvement of treatment planning system At JAEA (JCDS) for Boron Neutron Capture Therapy. International Conference on Advances in Nuclear Science and Engineering in Conjunction with LKSTN; November 2007; Bandung, Indonesia.
19. Lin TY, Liu YWH. Development and verification of THORplan-A BNCT treatment planning system for THOR. *Appl Radiat Isot.* 2011;69(12):1878-1881. doi:10.1016/j.apradiso.2011.03.025
20. Teng Y-C, Chen J, Zhong W-B, Liu Y-H. HU-based material conversion for BNCT accurate dose estimation. *Sci Rep.* 2023;13(1):15701. doi:10.1038/s41598-023-42508-0
21. Nakao M, Hayata M, Ozawa S, et al. Stoichiometric CT number calibration using three-parameter fit model for ion therapy. *Phys Medica.* 2022;99:22-30. doi:10.1016/j.ejmp.2022.05.005

22. Sato T, Iwamoto Y, Hashimoto S, et al. Features of Particle and Heavy Ion Transport code System (PHITS) version 3.02. *J Nucl Sci Technol*. 2018;55(6):684-690. doi:10.1080/00223131.2017.1419890
23. ICRP. *Adult reference computational phantoms*. ICRP; 2009;39(2).
24. Kanematsu N, Inaniwa T, Nakao M. Modeling of body tissues for Monte Carlo simulation of radiotherapy treatments planned with conventional x-ray CT systems. *Phys Med Biol*. 2016;61(13):5037-5050. doi:10.1088/0031-9155/61/13/5037
25. *Advances in Boron Neutron Capture Therapy*. International Atomic Energy Agency; 2023. <https://www.iaea.org/publications/15339/advances-in-boron-neutron-capture-therapy>
26. Shibata K, Iwamoto O, Nakagawa T, et al. JENDL-4.0: a new library for nuclear science and engineering. *J Nucl Sci Technol*. 2011;48(1):1-30. doi:10.1080/18811248.2011.9711675
27. Higashino M, Aihara T, Ozaki A, et al. Successful salvage surgery of the residual tumor after boron neutron capture therapy (BNCT): a case report. *Appl Radiat Isot*. 2022;189:110420. doi:10.1016/j.apradiso.2022.110420
28. Kawabata S, Suzuki M, Hirose K, et al. Accelerator-based BNCT for patients with recurrent glioblastoma: a multicenter phase II study. *Neuro-Oncology Adv*. 2021;3(1):1-9. doi:10.1093/noajnl/vdab067
29. Aihara T, Morita N, Kamitani N, et al. Boron neutron capture therapy for advanced salivary gland carcinoma in head and neck. *Int J Clin Oncol*. 2014;19(3):437-444. doi:10.1007/s10147-013-0580-3
30. Nakao M, Ozawa S, Miura H, et al. Development of a CT number calibration audit phantom in photon radiation therapy: a pilot study. *Med Phys*. 2020;47(4):1509-1522. doi:10.1002/mp.14077
31. Cropp RJ, Seslija P, Tso D, Thakur Y. Scanner and kVp dependence of measured CT numbers in the ACR CT phantom. *J Appl Clin Med Phys*. 2013;14(6):338-349. doi:10.1120/jacmp.v14i6.4417
32. Coxson HO. Sources of variation in quantitative computed tomography of the lung. *J Thorac Imaging*. 2013;28(5):272-279. doi:10.1097/RTI.0b013e31829efbe9
33. Sato H, Takata T, Suzuki M, Sakurai Y. Influence of lung physical density on dose calculation in boron neutron capture therapy for malignant pleural mesothelioma. *Appl Radiat Isot*. 2023;198:110857. doi:10.1016/j.apradiso.2023.110857
34. Balcerzyk M, De-Miguel M, Guerrero C, Fernandez B. Quantification of boron compound concentration for BNCT using positron emission tomography. *Cells*. 2020;9(9):2084. doi:10.3390/cells9092084
35. Isohashi K, Kanai Y, Aihara T, et al. Exploration of the threshold SUV for diagnosis of malignancy using 18F-FBPA PET/CT. *Eur J Hybrid Imaging*. 2022;6(1):35. doi:10.1186/s41824-022-00156-z
36. Rorer D, Wambersie G. Current status of neutron capture therapy. IAEA. 2001:7.

SUPPORTING INFORMATION

Additional supporting information can be found online in the Supporting Information section at the end of this article.

How to cite this article: Hu N, Nakao M, Ozawa S, et al. Application of stoichiometric CT number calibration method for dose calculation of tissue heterogeneous volumes in boron neutron capture therapy. *Med Phys*. 2024;51:4413–4422. <https://doi.org/10.1002/mp.17093>